

History, Progress and New Results in Synthetic Passive Element Design Employing CFTAs

Jaroslav Koton, Norbert Herencsar, and Martin Venclovsky

Abstract—After the presentation of the Current Follower Transconductance Amplifier (CFTA) active element, it has found a numerous application possibilities while designing linear and non-linear analog function blocks. This paper gives a short review of the CFTA and mainly focuses on the synthetic floating and grounded passive element design, which can also be electronically controllable. Except the design of synthetic inductors, also possible realizations of floating and grounded capacitors and resistors are described, where the value of these passive elements can be adjusted by means of active elements' parameters. For the design of the corresponding circuit realizations, the Mason-Coates signal flow graph approach is used. The performance of some discussed synthetic elements is verified and evaluated by Spice simulations on simple analog frequency filters.

Keywords—CFTA, synthetic inductor, synthetic capacitor, synthetic resistor, frequency filter, signal processing.

I. INTRODUCTION

Even if in these days the signal processing is mainly performed in the digital form, analog function blocks are still required in front-end interfaces. Probably the most discussed and used function blocks are the analog passive or active frequency filters, where in the literature more attention is paid to active ones. Although the mathematical description of these function blocks is very well known and the number of described circuit solutions using different types of active elements is also quite high, the engineers are still looking for new challenges if low supply voltage, low power consumption, or low noise are to be considered. Hence, new or modified active elements and new frequency filter design approaches are presented in the literature.

Once assuming the variety of active elements, probably the best known are the operational amplifiers (OPAs) and operational transconductance amplifiers (OTAs). These active elements are considered to be used in voltage mode (VM) function blocks, i.e. both the input and output variable to be voltage. However, other active elements suitable for the design of analog function blocks are discussed in the literature, such as Current Conveyors (CC) and their first generation - CCI [1], second generation - CCII [2] and third generation - CCIII [3], Voltage Conveyors (VC) [4] and their variants such as Current Differencing Buffered Amplifier (CDBA) [5] or Universal Voltage Conveyor (UVC) [6]. Even if these active

elements have both voltage and current input and/or output terminals, they are mostly used in function blocks working in the current mode (CM), where the input and output signal is represented by current. However, the character of the input and output variable of a function block does not have to be necessarily the same and hence mixed mode function blocks are designed that are described by a transadmittance or transimpedance transfer function. Interconnecting conveyors and/or voltage followers (VF) and/or current followers (CF) and operational transconductance amplifiers other types of active elements are presented in the literature with the aim of simpler internal transistor implementation. The Current-Differencing Transconductance Amplifier (CDTA) [7], Current Conveyor Transconductance Amplifier (CCTA) [8], Current Through Transconductance Amplifier (CTTA) [9] or Current Follower Transconductance Amplifier (CFTA) [10] can be given.

While presenting new types of active elements, their application possibilities are mostly shown on the design of frequency filters. For the design of linear functional blocks with these active elements, a number of methods can be used. The autonomous circuit method [11], [12], adjoint transformation [13], the use of passive prototype [14], or signal flow-graph approach [15] can be mentioned as examples.

This paper deals with the idea of designing synthetic elements that with advantage can be employed in passive filtering structures. For this purpose, the CFTA is used as active element for sake of the synthetic elements design. The paper is organized as follows: first, in section II the CFTA active element is described and possible realizations for practical verifications are given; next, in section III using signal flow graph approach, the circuit solutions of floating and grounded passive elements are discussed; in section IV, some of the synthetic elements are employed in simple function blocks to show their performance; section V concludes this paper and gives some views of future work in area of CFTA usage in analog signal processing blocks.

II. CFTA - CURRENT FOLLOWER TRANSCONDUCTANCE AMPLIFIER

A. Active Element Description

The Current Follower Transconductance Amplifier (CFTA) (Fig. 1(a)) is an analog active element that has been presented in [10] as a simplified version of the CDTA [7]. The simplification of CDTA to CFTA consists in the reduction of one low-impedance current input (n) as it can be seen from Fig. 1. The reason of such simplification was the fact that in

Manuscript received February 9, 2015; revised March 31, 2015.

J. Koton, N. Herencsar and M. Venclovsky are with Brno University of Technology, Faculty of Electrical Engineering and Communication, Dept. of Telecommunications, email: koton@feec.vutbr.cz

Research described in this paper was financed by the National Sustainability Program under grant LO1401. For the research, infrastructure of the SIX Center was used.



Fig. 1. Circuit symbols of (a) CFTA, (b) CDTA

numerous circuit solutions using CDТАs p or n terminals of individual active elements remain unconnected [7], [16]-[23] and hence can cause undesired noise injection into the circuit and subsequently increase the noise level at the output of the function block. Therefore, the CFTA uses only single low-impedance current input denoted as f , two high-impedance current outputs $x+$ and $x-$ and one auxiliary high-impedance voltage terminal z . The relation between the terminal currents and voltages of this active element can be described by following hybrid matrix:

$$\begin{bmatrix} v_f \\ i_z \\ i_{x+} \\ i_{x-} \end{bmatrix} = \begin{bmatrix} 0 & 0 & 0 & 0 \\ \alpha & 0 & 0 & 0 \\ 0 & g_m & 0 & 0 \\ 0 & -g_m & 0 & 0 \end{bmatrix} \begin{bmatrix} i_f \\ v_z \\ v_{x+} \\ v_{x-} \end{bmatrix}, \quad (1)$$

where $\alpha = 1 - \varepsilon$ is the current gain from the f terminal to the z terminal and g_m is the transconductance of the active element, whereas $|\varepsilon| \ll 1$ is the current tracking error. Generally, the g_m and α are frequency dependent, however for sake of simplicity, in following sections ideal values are assumed, i.e. g_m being constant and α being unity.

From the behavioral point of view, the CFTA can be represented as an interconnection of the Current Follower (CF) and Balanced-Output Transconductance Amplifier (BOTA) as it is shown in Fig. 2. The input of the current follower corresponds to the input terminal f of CFTA Fig. 2(a). The output of the current follower is interconnected with the negative voltage input of BOTA whereas this node also represents the auxiliary voltage input z . Based on the transconductance g_m of BOTA, the voltage at the z terminal is converted to corresponding currents i_{x+} and i_{x-} . Thanks to the usage of BOTA, there is a potential of the transconductance g_m being electronically tuned [24]. Therefore, the parameters of function blocks employing CFTA elements might be also tuned once proper CMOS implementation of the CFTA is used [25]. Based on the description of the behavior of the CFTA, its basic CMOS implementation can be used as shown in Fig. 2(b) [26]. Other possible CMOS or bipolar implementations of CFTA can be found e.g. in [27], [28].

In Fig. 3(a) possible implementation of CFTA using readily available integrated circuits is shown. Here, to implement the current follower, the current feedback amplifier AD844 [29] is used. The current follower can be also implemented using e.g. OPA861 [30]. The second part of CFTA represented by an OTA can be implemented using MAX435 [31]. Possible realization of a multiple-output CFTA (MO-CFTA) is shown in Fig. 3(b) [32], where the second generation current

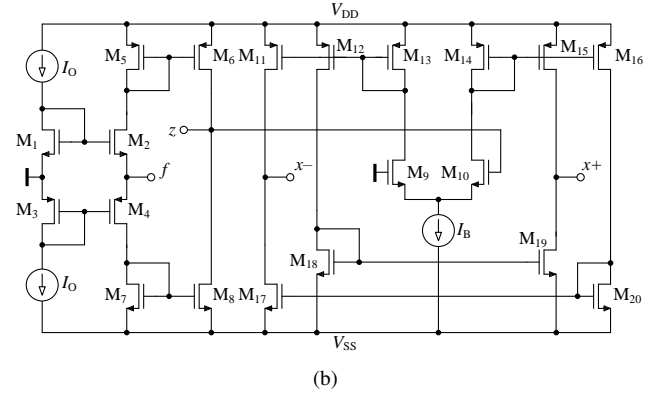


Fig. 2. Implementation of CFTA (a) interconnecting CF and BOTA, (b) CMOS implementation [26]

conveyor CCII+/- and Universal Current Conveyor (UCC) are used. Such interconnection is suitable for experimental measurements as the UCC together with CCII are part of the UCC-N1B integrated circuit, which in cooperation with Brno University of Technology has been designed by ON Semiconductor Ltd. [33], however, it is currently available only in laboratory samples. Note that in Fig. 3(b) using the Z_{S-} instead of Z_{S+} as an output terminal z , the MO-ICFTA (Multiple-Output Inverting CFTA) [34], which is also referred to as MO-CITA (Multiple-Output Current Inverter Transconductance Amplifier) [35], can be simply implemented using UCC-N1B.

B. Active Element Application Possibilities

Since the presentation of the CFTA, it has found its application possibilities in both linear and non-linear analog signal processing and function block design.

Mainly, it is employed in current- and voltage-mode multi-function frequency filters [10], [25], [27], [28], [32], [36]-[55]. E.g. in [32] three CFTAs are used to realize a current-mode single-input-multi-output second-order filter that features pole-frequency adjustment without varying quality factor of the pass-band gain. In the literature, research results that focus just on all-pass frequency filter design can be also found [56]-[60].

The proposed all-pass filters can be subsequently used for the design of oscillators as it is shown in [57] and [58]. However, the CFTA can be also used for direct quadrature and multi-phase oscillator design as presented in [61]-[67].

Assuming non-linear function blocks, the CFTA has been used to implement square-rooting circuits, multipliers, dividers, half-wave and full-wave rectifiers [68]-[72].

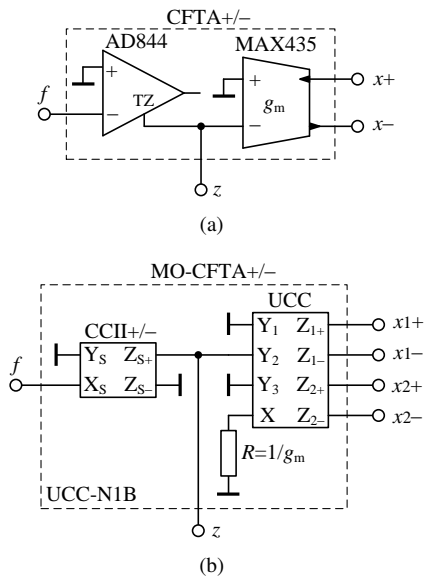


Fig. 3. Implementation of CFTA using (a) AD844 and MAX435, (b) Universal Current Conveyor (UCC)

Following the purpose of this paper, the current follower transconductance amplifier has found its application possibilities also in synthetic element design. The main focus is on the design of floating or grounded lossy or lossless inductor simulators [73]-[78]. In [73] using three CFTAs, the floating lossless inductor simulator is presented that can be easily used to design a grounded lossless inductor. Furthermore, in [73] using four active elements a floating capacitor simulator is presented. Simplifying the circuit solution of the floating inductor simulator from [73], the grounded lossless inductor using only two active elements and single grounded capacitor is presented in [74]. Using the V-I signal flow graph approach, the structure of grounded inductor simulator is presented in [75], which is, however, the same as in [74]. To reduce the number of active elements in floating lossless inductance simulator in [73], a modified version of CFTA, namely the Z-copy CFTA has been used. The structure in [76] uses only two active elements and single grounded capacitor, however, an external resistor is required. The grounded lossless inductor simulator of minimal configuration is presented in [77]. The solution is generally based on the circuit presented in [76], where the external resistor is now assumed to the intrinsic resistance of the active element - the CCCFTA (Current Controlled Current Follower Transconductance Amplifier). So far, the most complex paper dealing with the basic synthetic element design using CFTAs is [78], where the circuit solutions of inductor simulator, capacitance multiplier and also resistor simulator both floating and grounded are presented. However, in some cases the solutions presented in [78] operate only with ideal active elements. Following our previous results presented in [79], using the M-C signal flow graph approach, in this paper we present the design procedure of synthetic elements, where alternative and correct circuit solutions of basic synthetic elements are discussed.

III. FLOATING AND GROUNDED SYNTHETIC ELEMENTS DESIGN

While designing synthetic elements, the researchers mainly focus on the design of lossless or lossy grounded or floating synthetic inductor. The theory of synthetic elements can be further generalized where also other basic passive element interconnections can be realized using active elements to provide e.g. simple electronic adjustment of the designed function block's parameters.

Here, once designing floating and grounded synthetic passive element, not only the final circuit solutions are presented but also using the M-C signal flow representation of the passive components corresponding active circuit solution is determined.

A. M-C signal flow Graph Theory

Generally, a M-C signal flow graph is more used for sake of analysis of some known circuit rather than for a synthesis. However, e.g. in [15], the advantage of the signal flow graph design approach has been shown. To determine a relation or transfer function between two selected nodes (input X and output Y) in a graph the Mason's gain formula [80]:

$$K = \frac{Y}{X} = \frac{1}{\Delta} \sum_i P_i \Delta_i \quad (2)$$

should be used, where P_i is the transfer of the i th direct path from the input node X to the output node Y , and Δ is the determinant of the signal flow graph:

$$\Delta = V - \sum_k S_1^{(k)} V_1^{(k)} + \sum_l S_2^{(l)} V_2^{(l)} - \sum_l S_3^{(m)} V_3^{(m)} \dots, \quad (3)$$

where V is the product of the self-loops, $S_1^{(k)}$ is the transfer of the k th oriented loop and $V_1^{(k)}$ is the product of all self-loops not touching the k th oriented loop; $S_2^{(l)}$ is the transfer product of two mutually not touching oriented loops and $V_2^{(l)}$ is the product of the self-loops not touching the l th oriented loops. In case that an oriented loop or k th direct path is touching all nodes, then the product V or Δ_k is unity. In (2) Δ_i is the determinant of that part of the graph that is not touching the i th direct path.

It can be obvious that except the knowledge of the Mason's gain formula, it is also necessary to know the corresponding M-C graph of the active element. According to (1) the reduced M-C flow graph of the CFTA active element is shown in Fig. 4, where ideal behavior of the active element is assumed, i.e. $\alpha = 1$. In Fig. 4 Y_i represents the sum of admittances connected to the corresponding (i) terminal of the active element.

Based on the signal flow graph of the basic passive elements, and in some cases of their parallel interconnection, using the CFTA corresponding M-C flow graphs representing an active solution of the immittance simulator are determined.

B. Floating Lossless Inductor Simulator

To define the equivalent active solution of a floating inductor, the general admittances Y_A and Y_B are used as shown in Fig. 5. These general admittances represent parts of the circuit

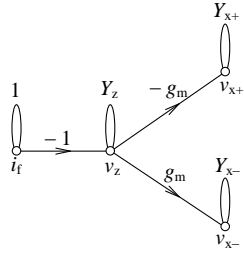


Fig. 4. Reduced M-C signal flow graph of CFTA+/-

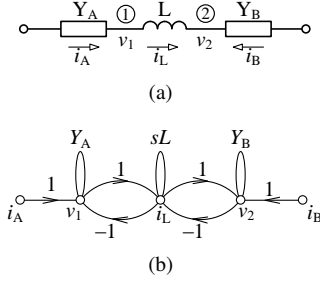


Fig. 5. (a) Floating passive inductor connected in a circuit (represented by admittances \$Y_A\$ and \$Y_B\$), (b) corresponding signal flow graph

that are interconnected with the inductor. In the corresponding signal flow graph (Fig. 5(b)), the general admittances at the input and output of the inductor are present only to show their influence on the gain of the corresponding self-loops. Using (2) following transfer function can be obtained:

$$\frac{v_1}{i_B} = \frac{v_2}{i_A} = \frac{1}{sLY_A Y_B + Y_A + Y_B}, \quad (4)$$

which generally corresponds to a floating element.

Before presenting the determined signal flow graph of the active inductor simulator, it is suitable to shortly describe the features of the signal flow graph from Fig. 5(b). Once assuming the input and output node according to (4) there is only single direct path between these nodes and the signal flow graph consists only of two mutually touching oriented loops. Such properties should also feature the signal flow graph of the inductance simulator using CFTAs.

In Fig. 6(a) the signal flow graph of the active lossless floating inductor simulator is shown. This signal flow graph also generally consists of two mutually touching oriented loops and the using (2) the transfer function can be found as:

$$\frac{v_{z3}}{i_A} = \frac{g_{m1}g_{m2}}{sC_L Y_A Y_B + Y_A g_{m2}g_{m3} + Y_B g_{m1}g_{m2}}, \quad (5a)$$

$$\frac{v_{z1}}{i_B} = \frac{g_{m2}g_{m3}}{sC_L Y_A Y_B + Y_A g_{m2}g_{m3} + Y_B g_{m1}g_{m2}}, \quad (5b)$$

which in general corresponds to (4) and once we assume:

$$C_L = Lg_{m1}g_{m2}, \quad (6)$$

while \$g_{m1} = g_{m3}\$ then (4) and (5) become identical. According to Fig. 6(a) the circuit representation of the floating inductor simulator using three CFTAs (being identical with the solution

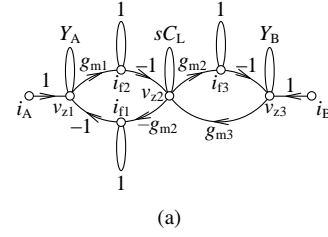


Fig. 6. (a) Signal flow graph of the floating inductor simulator using CFTAs, (b) circuit representation

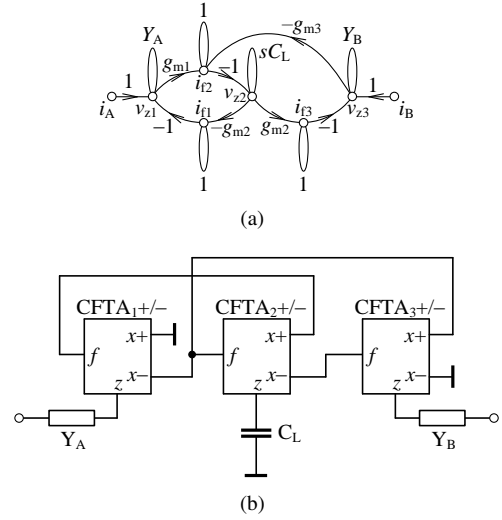


Fig. 7. Optimized solution of the floating inductor simulator using CFTAs: (a) signal flow graph, (b) circuit representation

presented in [78]) is shown in Fig. 6(b), whereas the equivalent inductance is determined as:

$$L_{eq} = \frac{C_L}{g_{m1}g_{m2}}, \quad (7)$$

once \$g_{m1} = g_{m3}\$.

The structure of the floating inductor simulator in Fig. 6 can be further optimized as it is shown in Fig. 7. In practice this optimization results in better performance of the inductor simulator at higher frequencies as the capacitor \$C_L\$ is connected only to the \$z\$ terminal of CFTA₂.

C. Grounded Lossless Inductor Simulator

The circuit solution of an grounded lossless inductor simulator can be determined from Fig. 6 or Fig. 7. Using the signal flow graph approach, the assumed representation of a passive inductor connected to a circuit together with the corresponding signal flow graph is shown in Fig. 8.

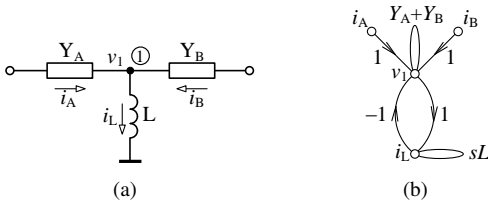


Fig. 8. (a) Grounded passive inductor connected in to a circuit, (b) corresponding signal flow graph

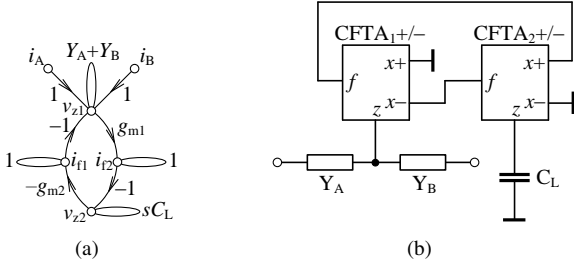


Fig. 9. (a) Signal flow graph of the grounded inductor simulator using CFTAs, (b) circuit representation

The transfer function of the signal flow graph is:

$$\frac{v_1}{i_B} = \frac{sL}{sL(Y_A + Y_B) + 1}. \quad (8)$$

Following the features of the signal flow graph from Fig. 8(b), signal flow graph using active elements can be defined as shown in Fig. 9(a). The transfer function of signal flow graph of the grounded inductor simulator can be determined as:

$$\frac{v_{z1}}{i_B} = \frac{sC_L}{sC_L(Y_A + Y_B) + g_{m1}g_{m2}}. \quad (9)$$

Assuming (6), then (9) and (8) become identical and hence the circuit solution in Fig. 9(b) represents an active simulator of a grounded lossless inductor with the equivalent inductance given by (7).

D. Floating Capacitor Multiplier

Generally, it is not difficult to produce neither grounded or floating capacitor in the integrated form nowadays. However, based on the technology used the capacitance of such capacitors is limited to tents of pF. Therefore, capacitor multipliers are useful function blocks once higher capacitances have to be used. Furthermore, using suitable active elements, the value of the capacitor can be easily adjusted, if required.

To derive the active floating capacitor multiplier, a floating capacitor C is assumed as shown in Fig. 10. The transfer function of the signal flow graph from Fig. 10(b) can be determined as:

$$\frac{v_1}{i_B} = \frac{v_2}{i_A} = \frac{sC}{sCY_A + sCY_B + Y_A Y_B}. \quad (10)$$

As it is obvious from Fig. 10(b) the signal flow graph has only single oriented loop with the gain s^2C^2 , which is typical for floating passive elements represented as admittances in

a graph. Therefore, to avoid the use of a floating capacitor in the active capacitor multiplier and still obtain the transfer function sufficient number of terms, the signal flow graph must contain of three mutually touching loops and furthermore, the corresponding signal flow graph must contain a high-impedance node, which in Fig. 11(a) is characterized by zero self-loop gain.

The transfer characteristic of the signal flow graph from Fig. 11(a) is:

$$\frac{v_{z3}}{i_A} = \frac{sC_g g_{m1} g_{m2}}{sC_g g_{m2}(Y_A g_{m3} + Y_B g_{m1}) + Y_A Y_B g_{m4} g_{m5}}, \quad (11a)$$

$$\frac{v_{z1}}{i_B} = \frac{sC_g g_{m2} g_{m3}}{sC_g g_{m2}(Y_A g_{m3} + Y_B g_{m1}) + Y_A Y_B g_{m4} g_{m5}}. \quad (11b)$$

Comparing (10) and (11) the equivalent value of the floating capacitor can be determined as:

$$C_{eq} = \frac{g_{m1} g_{m2}}{g_{m4} g_{m5}} C_g, \quad (12)$$

while it must hold $g_{m1} = g_{m3}$.

Comparing the circuit solution of the capacitor multiplier from Fig. 11(b) (or its signal flow graph in Fig. 11(a)) to the floating inductor simulator from Fig. 6(b) and the grounded inductor simulator from Fig. 9(b) it can be observed that the capacitor multiplier represents an interconnection of the floating inductor simulator, where instead of a capacitor C_L the grounded inductor simulator is connected. This feature fully corresponds to the circuit theory, e.g. [81].

Similarly, as the floating inductor simulator has been optimized, also an optimized solution of the capacitor multiplier can be described as shown in Fig. 12(b). Furthermore, using MO-CFTA, the number of active elements could be limited by one. This optimization step can be more obvious from the signal flow graph in Fig. 12(a) that has the transfer function defined as:

$$\frac{v_{z3}}{i_A} = \frac{sC_g g_{m1} g_{m2}}{sC_g g_{m2}(Y_A g_{m3} + Y_B g_{m1}) + Y_A Y_B g_{m2} g_{m4}}, \quad (13a)$$

$$\frac{v_{z1}}{i_B} = \frac{sC_g g_{m2} g_{m3}}{sC_g g_{m2}(Y_A g_{m3} + Y_B g_{m1}) + Y_A Y_B g_{m2} g_{m4}}. \quad (13b)$$

Subsequently, using the optimized circuit solution from Fig. 12(b) for the equivalent value of the floating capacitor it holds:

$$C_{eq} = \frac{g_{m1}}{g_{m4}} C_g, \quad (14)$$

whereas $g_{m1} = g_{m3}$.

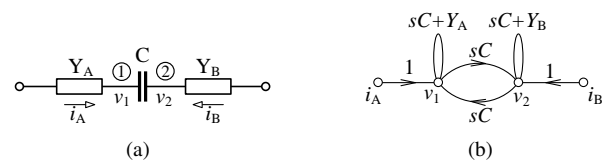


Fig. 10. (a) Floating passive capacitor connected in to an external circuit, (b) corresponding signal flow graph

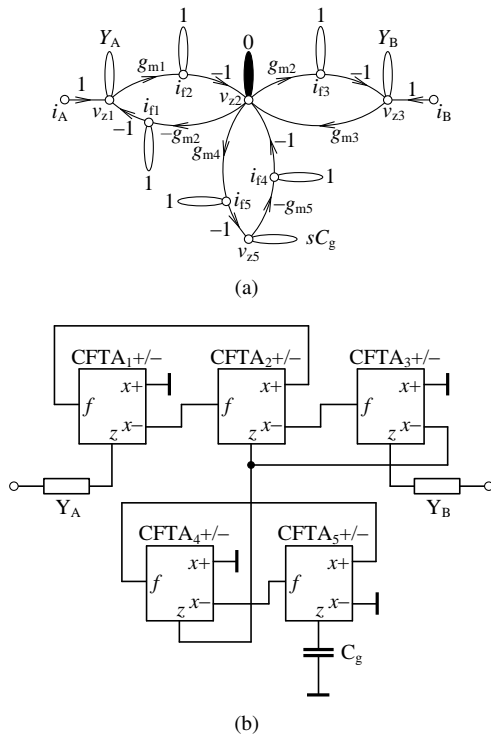


Fig. 11. (a) Signal flow graph of the floating capacitor multiplier using CFTAs, (b) circuit representation

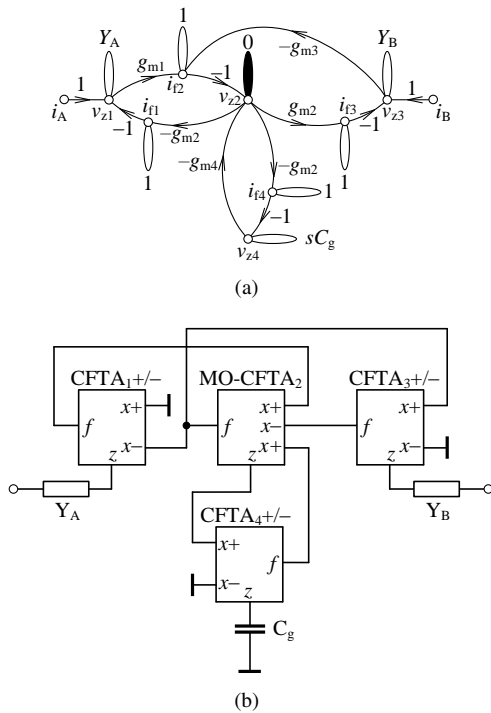


Fig. 12. Optimized solution of the floating capacitor multiplier: (a) signal flow graph, (b) circuit representation

A capacitance multiplier using three CFTAs and one MO-CFTA is also presented in [78]. As shown in Fig. 13(a), in this solution only the OTA part of the two active elements is used. As the current follower part of CFTA₂ and CFTA₄ is

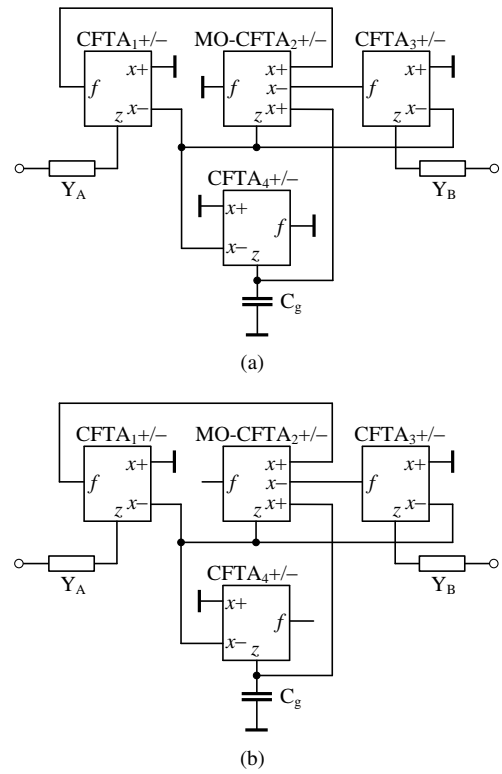


Fig. 13. (a) Floating capacitor multiplier from [78] with grounded f terminals, (b) correct solution with f terminals being floating

not employed the authors connect the current input terminals f to the ground. Such treatment of unused ports of the active element has no influence on the behavior of the function block once ideal active elements are assumed. However, in practice the unused f terminals must be left open to ensure current i_f being zero as shown in Fig. 13(b) or should be used as functional as shown in Fig. 12(b). Note that the notation (polarity) of the x terminals in Fig. 13(a) differ from the notation used in the original solution presented in [78], which is caused by different active element description used in [78].

E. Grounded Capacitor Multiplier

Once employing synthetic inductors or any other synthetic element in the designed structure of a function block that using active elements can be tuned, simple passive capacitors generally do not need to be implemented using active elements. However, for sake of completeness, we also present the grounded capacitor multiplier that can be used if required.

Using signal flow graph, the grounded passive capacitor connected to a circuit can be represented as shown in Fig. 14. The transfer function of the graph can be determined as:

$$\frac{v_1}{i_A} = \frac{1}{sC + Y_A + Y_B}. \quad (15)$$

The signal flow graph of the grounded capacitor multiplier can be derived from the signal flow graph from Fig. 11(a), where the one oriented loop has been omitted as it can be obvious in Fig. 15(a). For the transfer function of this graph it

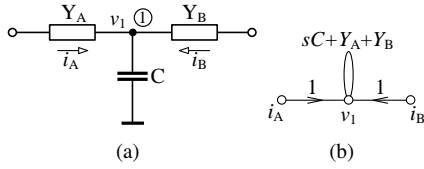


Fig. 14. (a) Grounded passive capacitor connected to a circuit, (b) corresponding signal flow graph

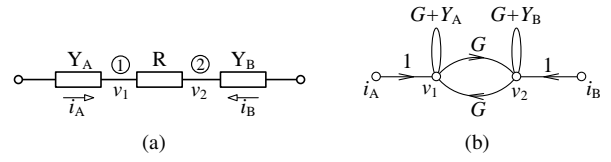


Fig. 16. (a) Floating passive resistor connected to a circuit, (b) corresponding signal flow graph

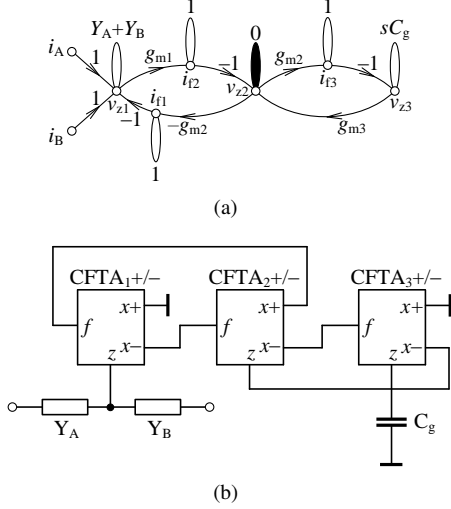


Fig. 15. (a) Signal flow graph of the grounded capacitor multiplier using CFTAs, (b) corresponding circuit representation

holds:

$$\frac{v_{z1}}{i_A} = \frac{g_{m2}g_{m3}}{g_{m1}g_{m2}sC_g + g_{m2}g_{m3}(Y_A + Y_B)} \quad (16)$$

Comparing (16) and (15) the equivalent value of the grounded capacitor equals to:

$$C_{eq} = \frac{g_{m1}}{g_{m3}}C_g, \quad (17)$$

and the circuit realization of the grounded capacitor multiplier using three CFTAs is shown in Fig. 15(b).

F. Floating Resistor Simulator

Using the CFTAs a floating resistor simulator can also be easily implemented. Following the theoretical background presented in previous sections, the passive resistor \$R\$ is connected to a circuit represented by general admittances \$Y_A\$ and \$Y_B\$ as shown in Fig. 16(a). In the corresponding signal flow graph, the resistor is expressed by its conductivity \$G\$ (Fig. 16(b)) and the transfer function of this graph is given as:

$$\frac{v_1}{i_B} = \frac{v_2}{i_A} = \frac{G}{GY_A + GY_B + Y_A + Y_B} \quad (18)$$

Similarly as in case of the floating capacitor multiplier, the signal flow graph of the active resistor simulator cannot be determined directly. To design an active floating resistor simulator two CFTAs are used that in the signal flow graph create three oriented loops as shown in Fig. 17(a). The transfer functions of this graph are:

$$\frac{v_{z2}}{i_A} = \frac{g_{m1}}{g_{m2}Y_A + g_{m1}Y_B + Y_A Y_B}, \quad (19a)$$

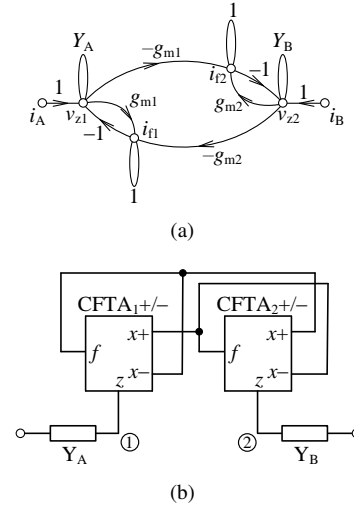


Fig. 17. (a) Signal flow graph of the floating resistor simulator using CFTAs, (b) corresponding circuit representation

$$\frac{v_{z1}}{i_B} = \frac{g_{m2}}{g_{m2}Y_A + g_{m1}Y_B + Y_A Y_B} \quad (19b)$$

Comparing (18) and (19) it is evident that it must hold \$g_{m1} = g_{m2} = g_m\$ and the equivalent value of the floating resistor equals to:

$$R_{eq} = \frac{1}{g_m} \quad (20)$$

The corresponding representation of the floating resistor simulator is shown in Fig. 17(b).

G. Grounded Resistor Simulator

From the basic passive elements, also the grounded resistor can be implemented using active elements. The representation of a passive resistor connected into a circuit and the corresponding part of the signal flow graph is shown in Fig. 18. The transfer function of the signal flow graph from Fig. 18(b) is given as:

$$\frac{v_1}{i_A} = \frac{1}{G + Y_A + Y_B} \quad (21)$$

The signal flow graph featuring the same transfer function using active elements can be determined from Fig. 17(a) by proper simplification as shown in Fig. 19(a). This signal flow graph contains only single oriented loop and for its transfer function it holds:

$$\frac{v_z}{i_A} = \frac{1}{Y_A + Y_B + g_m} \quad (22)$$

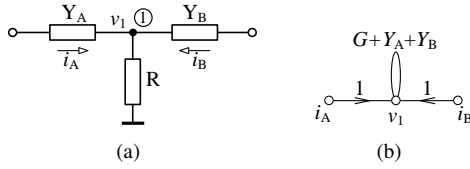


Fig. 18. (a) Grounded passive resistor connected to a circuit, (b) corresponding signal flow graph

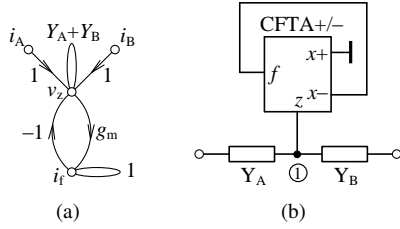


Fig. 19. (a) Signal flow graph of the grounded resistor simulator using CFTA, (b) corresponding circuit representation

The circuit solution using single CFTA is shown in Fig. 19(b) with the equivalent resistance given by (20).

As shown, using the signal flow graph approach it is possible to design active representation of passive elements, both floating and grounded, which can be with advantage used e.g. for frequency filter design that is based on a passive prototype.

IV. APPLICATION OF PROPOSED SYNTHETIC ELEMENTS

To show the operation and functionality of the proposed synthetic elements described in previous section, some of them are used in simple frequency filters. All the circuits presented in this section were simulated using Spice, whereas the CFTA has been implemented using the UCC-N1B model as shown in Fig. 3(b).

A. Low-pass Frequency Filter

In Fig. 20 the second-order low-pass filter is shown. Here, the floating inductor L is replaced by the corresponding active inductor simulator from Fig. 6(b) and also by active inductor simulator from Fig. 7(b) as shown in Fig. 21.

For the transfer function of the passive prototype from Fig. 20 it holds:

$$K_{pas} = \frac{G}{s^2 LCG + sC + G}. \quad (23)$$

and the transfer function of the active filters from Fig. 21 can be determined as:

$$K_{act} = \frac{Gg_{m1}g_{m2}}{s^2 C_L C G + sCg_{m1}g_{m2} + Gg_{m2}g_{m3}}, \quad (24)$$

whereas it must hold $g_{m1} = g_{m3}$.

The quality factor Q and angular pole-frequency ω_0 are:

$$Q = G\sqrt{\frac{L}{C}} = G\sqrt{\frac{C_L}{C} \frac{1}{g_{m1}g_{m2}}}, \quad (25a)$$

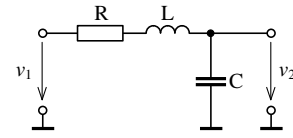


Fig. 20. Passive prototype of low-pass filter

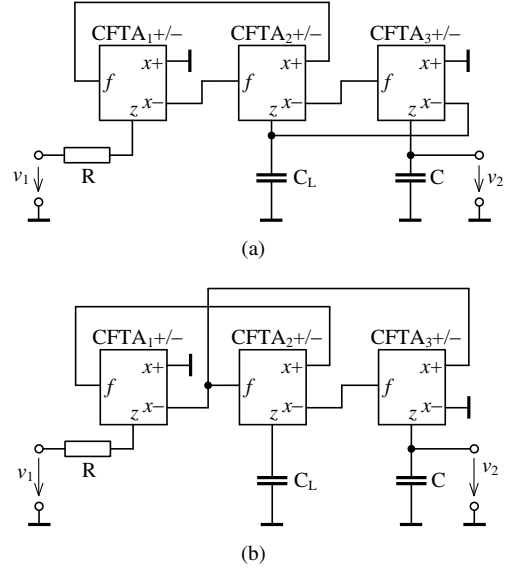


Fig. 21. Active low-pass frequency filter; floating inductor replaced by inductor simulator (a) from Fig. 6(b), (b) from Fig. 7(b)

$$\omega_0 = 2\pi f_0 = \frac{1}{\sqrt{LC}} = \sqrt{\frac{g_{m1}g_{m2}}{C_L C}}. \quad (25b)$$

Using (25), for $Q = 0.707$ and $f_0 = 100$ kHz, the values of passive elements can be determined as: $R = 1$ k Ω , $C = 2.2$ nF and $L = 1$ mH. According to (7), for the active filter we can select $C_L = 2.2$ nF, $g_{m1} = g_{m3} = 1/820$ S and $g_{m2} = 1/560$ S. The simulation results of the transfer function magnitude are shown and compared in Fig. 22. It is evident that the magnitudes are nearly the same hence, the behavior of the floating inductor simulators is correct.

B. High-pass Frequency Filter

The use of the grounded loss-less inductor simulator from Fig. 9(b) is shown on the design of high-pass filter. The passive prototype of the filter is in Fig. 23(a) and the corresponding solution using CFTAs is in Fig. 23(b).

The voltage transfer function of the passive and active high-pass filter are:

$$K_{pas} = \frac{s^2 LCG}{s^2 LCG + sC + G}, \quad (26a)$$

$$K_{act} = \frac{s^2 C_L C G}{s^2 C_L C G + sCg_{m1}g_{m2} + Gg_{m1}g_{m2}}, \quad (26b)$$

respectively.

The quality factor Q and the angular pole-frequency ω_0 equal to (25). Hence, for $Q = 0.707$ and $f_0 = 100$ kHz,

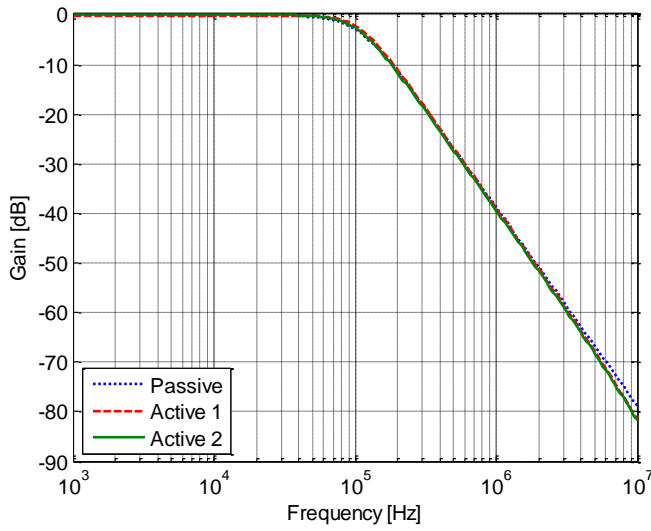


Fig. 22. Magnitude of the low-pass filters from Fig. 20 (Passive), Fig. 21(a) (Active 1) and Fig. 21(b) (Active 2)

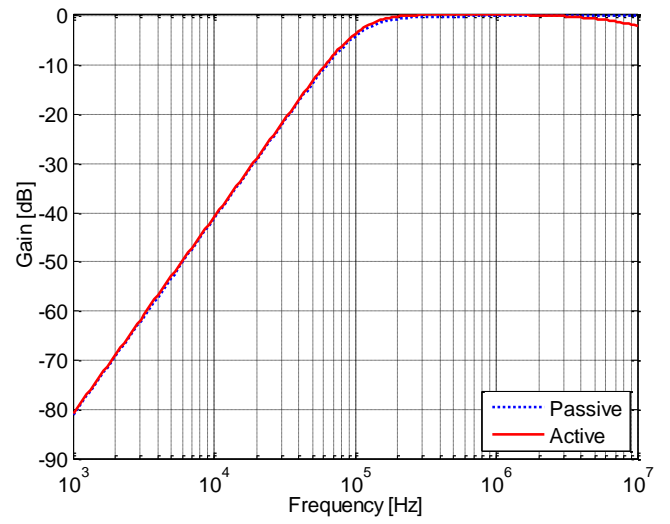


Fig. 24. Magnitude of the high-pass filters from Fig. 23

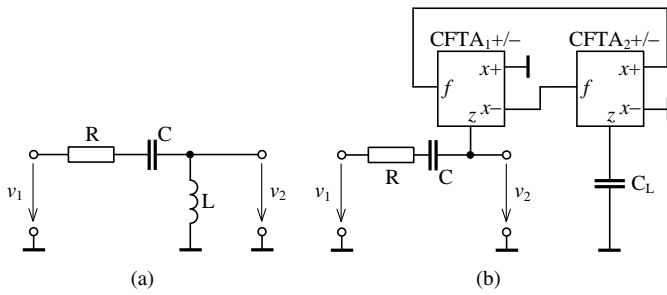


Fig. 23. High-pass frequency filter: (a) passive prototype, (b) filter using inductance simulator from Fig. 9(b)

the values of the passive are $R = 1 \text{ k}\Omega$, $C = 2.2 \text{ nF}$ and $L = 1 \text{ mH}$. According to (7), for the active filter we can select $C_L = 2.2 \text{ nF}$, $g_{m1} = g_{m3} = 1/820 \text{ S}$ and $g_{m2} = 1/560 \text{ S}$. The simulation results of the transfer function magnitude of the passive and active filter solution are shown and compared in Fig. 24. Also here, the magnitudes for the passive and active are nearly the same, which confirms the operability of the inductor simulator. Due to the frequency limitations of the active elements used, which is approx. 30 MHz [33], the gain of the active high-pass filter drops. The affect of the active elements at high frequencies can be also observed in case of the low-pass filter (Fig. 22), however, the higher attenuation in this frequency range is not detrimental.

C. Band-pass Frequency Filter

To show the operation of the floating capacitor multiplier from Fig. 12(b) it has been used to design a band-pass filter according to the passive prototype from Fig. 25(a). The transfer function of the passive filter is:

$$K_{pas} = \frac{sC}{sLCG + sC + G}. \quad (27)$$

To present the performance only of the capacitor multiplier, the floating inductor has not been replaced by its proper

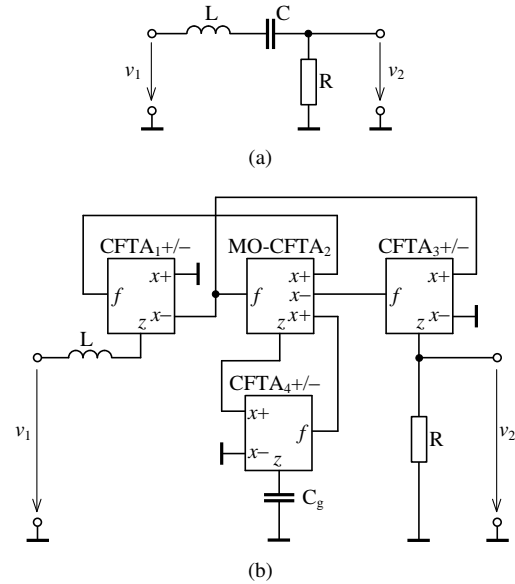


Fig. 25. Band-pass frequency filter: (a) passive prototype, (b) filter using capacitor multiplier from Fig. 12(b)

simulator and the final active band-pass filter is shown in Fig. 25(b). The transfer function of the filter is:

$$K_{act} = \frac{sC_g g_{m1} g_{m2}}{s^2 LC_g G g_{m1} g_{m2} + sC_g g_{m2} g_{m3} + G g_{m2} g_{m4}}. \quad (28)$$

The quality factor Q and the angular pole-frequency ω_0 of the band-pass filters from Fig. 25 are:

$$Q = G \sqrt{\frac{L}{C}} = \frac{G}{g_{m3}} \sqrt{\frac{L g_{m1} g_{m4}}{C_g}}, \quad (29a)$$

$$\omega_0 = \frac{1}{\sqrt{LC}} = \sqrt{\frac{g_{m4}}{LC_g g_{m1}}}. \quad (29b)$$

Using (29), for $Q = 0.707$ and $f_0 = 100 \text{ kHz}$, the values of passive elements are $R = 1 \text{ k}\Omega$, $C = 2.2 \text{ nF}$ and $L = 1 \text{ mH}$. In case of the filter using capacitor multiplier, according to (12)

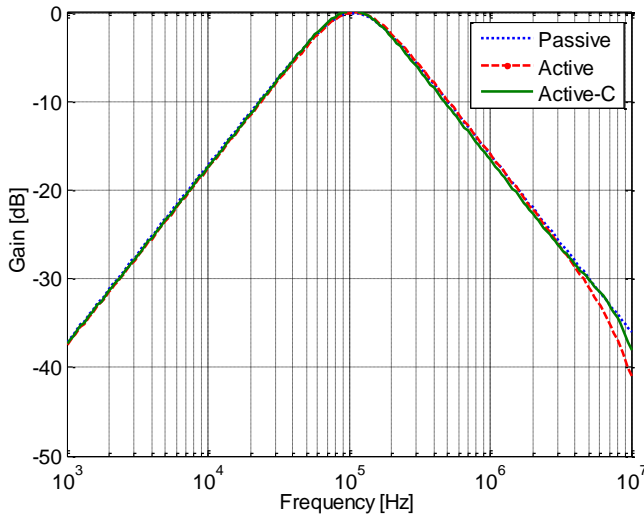


Fig. 26. Magnitude of the band-pass filters from Fig. 25(a) (Passive), from Fig. 25(b) (Active), and from Fig. 27 (Active-C)

the following values selected: $g_{m1} = g_{m2} = g_{m3} = 1$ mS, $g_{m4} = 1/2.2$ mS, and $C_g = 1$ nF to obtain the equivalent value of the floating capacitor C . The simulation results of the band-pass filter are shown in Fig. 26. Based on the results, also in this case it can be stated that the behavior of the proposed floating capacitor multiplier corresponds to the theoretical presumptions. Similarly as in previous cases, at higher frequencies the affect of the active elements can be observed as the attenuation is higher than it is for passive filter. Anyway, in this case such behavior also does not represent a problem.

D. Active-C Band-pass Filter

In previous subsection dealing with the design of band-pass filter, only the floating capacitor has been replaced by its synthetic element (Fig. 25(b)). However, in the passive prototype from Fig. 25(a) (and actually in any other passive circuit), all the passive elements can be replaced by their corresponding active solution presented in section III. Hence, active-C band-pass filter can be proposed as shown in Fig. 27 (see next page) that is described by the following transfer function:

$$K_{active-C} = \frac{sC_g g_{mC1} g_{mL1} g_{mL2}}{s^2 C_L C_g g_{mC1} g_{mR} + sC_g g_{mC1} g_{mL1} g_{mL2} + g_{mL1} g_{mL2} g_{mR} g_{mC4}}, \quad (30)$$

whereas according to synthetic elements solutions described in section III $g_{mC1} = g_{mC3}$ and $g_{mL1} = g_{mL3}$.

Similarly to the previous cases, the angular pole-frequency ω_0 and quality factor Q of the active-C band pass filter can be defined:

$$\omega_0 = \sqrt{\frac{g_{mL1} g_{mL2} g_{mC4}}{C_L C_g g_{mC1}}}, \quad (31a)$$

$$Q = g_{mR} \sqrt{\frac{C_L}{C_g}} \sqrt{\frac{g_{mC4}}{g_{mC1} g_{mL1} g_{mL2}}}. \quad (31b)$$

Using (31), for $Q = 0.707$ and $f_0 = 100$ kHz, the parameters of the active elements are as follows: $g_{mL1} = g_{mL3} = 1/820$ S, $g_{mL2} = 1/560$ S, $g_{mC1} = g_{mC2} = g_{mC3} = 1$ mS, $g_{mC4} = 1/2.2$ mS, and $g_{mR} = 1$ mS. The values of the two grounded capacitors are $C_L = 2.2$ nF and $C_g = 1$ nF. The simulation results of the transfer function magnitude of the active-C band-pass filter from Fig. 27 are shown in Fig. 26. Here, the behavior of the active-C filter can be compared with the passive filter from Fig. 25(a) and band-pass filter from Fig. 25(b), where only the floating capacitor has been replaced by the corresponding floating capacitor multiplier. As it can be seen, also the properties of active-C filter are satisfactory and agree very well to theoretical presumptions.

V. CONCLUSION

In this paper, a short overview of application possibilities of the current follower transconductance amplifier (CFTA) active element has been presented. The main attention has been paid to the use of this active element for synthetic element design. Using the signal flow graph approach, except the design of synthetic inductors, also possible realizations of floating and grounded capacitors and resistors were described, where the value of these passive elements can be adjusted by means of active elements parameters. The performance of the selected synthetic elements has been shown on the design of simple frequency filters. The obtained simulation results show that the proposed structures are suitable for active-only frequency filter design, where only grounded capacitors are used.

REFERENCES

- [1] K. C. Smith, A. Sedra, "The current conveyor: a new circuit building block," *IEEE Proc.*, vol. 56, pp. 1368–1369, 1968.
- [2] A. Sedra, K. C. Smith, "A second-generation current conveyor and its application," *IEEE Trans. Circuit Theory*, vol. 17, pp. 132–134, 1970.
- [3] A. Fabre, "Third-generation current conveyor: a new helpful active element," *Electronics Letters*, vol. 31, no. 5, pp. 338–339, 1995.
- [4] T. Dostal, J. Pospisil, "Current and voltage conveyors - a family of three port immittance converters," *Proc. ISCAS, Roma*, pp. 419–422, 1982.
- [5] C. Acar, S. Ozoguz, "A new versatile building block: current differencing buffered amplifier suitable for analog signal-processing filters," *Microelectronics Journal*, vol. 30, no. 2, pp. 157–160, 1999.
- [6] J. Koton, K. Vrba, N. Herencsar, "Tunable filter using voltage conveyors and current active elements," *Int. J. Electronics*, vol. 96, no. 8, pp. 787–794, 2009.
- [7] D. Biolek, "CDTA - Building Block for Current-Mode Analog Signal Processing," in *Proc. Int. Conf. ECCTD03 Krakow, Poland*, vol. III, pp. 397–400, 2003.
- [8] R. Prokop, V. Musil, "CCTA-a new modern circuit block and its internal realization," in *Proc. Int. Conf. Electronic Devices and Systems*, pp. 89–93, Brno, Czech Republic, 2005.
- [9] D. Biolek, V. Biolkova, "CTTA Current-mode filters based on current dividers," in *Proc. 11th Electronic Devices and Systems Conference*, pp. 2–7, 2004.
- [10] N. Herencsar, J. Koton, I. Lattenberg, K. Vrba, "Signal-flow Graphs for Current-Mode Universal Filter Design Using Current Follower Transconductance Amplifiers (CFTAs)," in *Proc. Int. Conf. Applied Electronics - APPEL, Pilsen, Czech Republic*, pp. 69–72, 2008.
- [11] C. Hou, Y. Wu, S. Liu, "New configuration for single-CCII first-order and biquadratic current mode filters," *Int. J. Electronics*, vol. 71, no. 4, pp. 637–644, 1991.
- [12] K. Vrba, J. Cajka, V. Zeman, "New RC-Active Network Using Current Conveyors," *Radioengineering*, vol. 6, no. 2, pp. 18–21, 1997.
- [13] G. W. Roberts, A. S. Sedra, "All Current-mode Frequency Selective Filters," *Electronics Letters*, vol. 25, no. 12, pp. 759–760, 1989.

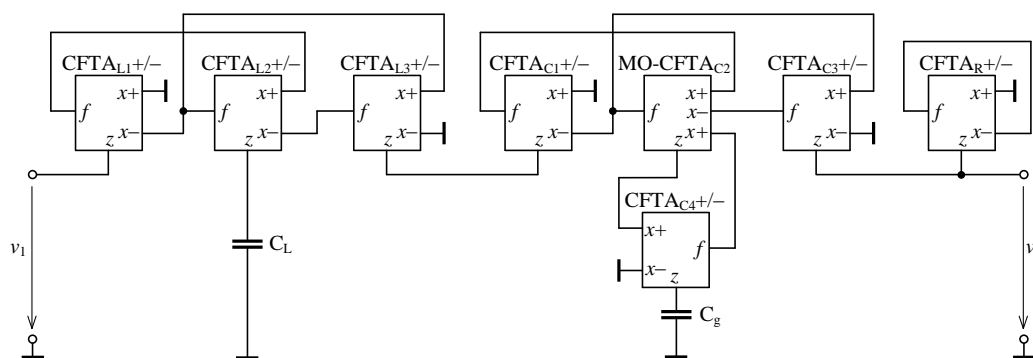


Fig. 27. Active-C band-pass filter based on the passive prototype from Fig. 25(a)

- [14] Y.-S. Hwang, P.-T. Hung, W. Chen, S.-I. Liu, "CCII-based linear transformation elliptic filters," *Int. J. Electronics*, vol. 89, no. 2, pp. 123–133, 2002.
- [15] J. Koton, K. Vrba, P. Ushakov, J. Misurec, "Designing Electronically Tunable Frequency Filters Using the Signal Flow Graph Theory," in *Proc. 31th Int. Conf. Telecommunications and Signal Processing - TSP*, pp. 41–43, 2008.
- [16] A. Uygur, H. Kuntman, A. Zeki, "Multi-input multi-output CDTA-based KHN filter," in *Proc. 4th Int. Conf. Electrical and Electronics*, Bursa, Turkey, 2005.
- [17] A. U. Keskin, D. Biolek, E. Hancioglu, V. Biolkova, "Current-mode KHN filter employing current differencing transconductance amplifiers," *Int. J. Electronics and Communications*, vol. 60, no. 6, pp. 443–446, 2006.
- [18] N. A. Shah, M. Quadri, S. Z. Iqbal, "Realization of CDTA based current-mode universal filter," *Indian Journal of Pure and Applied Physics*, vol. 46, no. 4, pp. 283–285, 2008.
- [19] D. Biolek, V. Biolkova, Z. Kolka, "Current-mode biquad employing single CDTA," *Indian Journal of Pure and Applied Physics*, vol. 47, no. 7, pp. 535–537, 2009.
- [20] A. Lahiri, "New current-mode quadrature oscillators using CDTA," *IEICE Electronics Express*, vol. 6, no. 3, pp. 135–140, 2009.
- [21] D. Prasad, D. R. Bhaskar, A. K. Singh, "New grounded and floating simulated inductance circuits using current differencing transconductance amplifiers," *Radioengineering*, vol. 19, no. 1, pp. 194–198, 2010.
- [22] W. Tangsrirat, T. Pukkalanun, P. Mongkolwai, and W. Surakampon-torn, "Simple current-mode analog multiplier, divider, square-roter and squarer based on CDTAs," *Int. J. Electronics and Communications*, vol. 65, no. 3, pp. 198–203, 2011.
- [23] L. Tan, K. Liu, Y. Bai, J. Teng, "Construction of CDDBA and CDTA behavioral models and the applications in symbolic circuits analysis," *Analog. Integr. Circ. Sig. Process.*, vol. 75., no. 3, pp. 517–523, 2013.
- [24] R. L. Geiger, E. Snchez-Sinencio, "Active Filter Design Using Operational Transconductance Amplifiers: A Tutorial," *IEEE Circuits and Devices Magazine*, Vol. 1, pp. 20–32, 1985.
- [25] N. Herencsar, J. Koton, K. Vrba, A. Lahiri, O. Cicekoglu, "Current-Controlled CFTA-Based Current-Mode SITO Universal Filter and Quadrature Oscillator," in *Proc. Int. Conf. Applied Electronics - APPEL*, Pilsen, Czech Republic, pp. 121–124, 2010.
- [26] N. Herencsar, J. Koton, K. Vrba, O. Cicekoglu, "New Active-C Grounded Positive Inductance Simulator Based on CFTAs," in *Proc. Int. Conf. Telecommunications and Signal Processing - TSP*, pp. 35–37, 2010.
- [27] P. Suwanjan, W. Jaikla, "CFTA Based MISO Current-mode Biquad Filter," in *Proc. Recent Researches in Circuits, Systems, Multimedia and Automatic Control*, Rovaniemi, Finland, pp. 93–97, 2012.
- [28] W. Tangsrirat, "Active-C Realization of nth-order Current-Mode Allpole Lowpass Filters Using CFTAs," in *Proc. Int. MultiConf. Engineers and Computer Scientists - IMECS*, vol. II, pp. 1–4, 2012.
- [29] Datasheet AD844: 60 MHz 2000 V/ μ s Monolithic Op Amp, Analog Devices, Rev. 7, 2009.
- [30] Datasheet OPA861: Wide Bandwidth Operational Transconductance Amplifier (OTA), Texas Instruments, SBOS338G, 2013.
- [31] Datasheet MAX435/MAX436: Wideband Transconductance Amplifiers, MAXIM, Rev. 1, 1993.
- [32] N. Herencsar, J. Koton, K. Vrba, J. Misurec, "A Novel Current-Mode SIMO Type Universal Filter Using CFTAs," *Contemporary Engineering Sciences*, vol. 2, no. 2, pp. 59–66, 2009.
- [33] Datasheet UCC-N1B: Universal Current Conveyor (UCC) and Second-Generation Current Conveyor (CCII+/-), ON Semiconductor & Brno University of Technology, Rev. 1, 2010.
- [34] N. Herencsar, J. Koton, K. Vrba, I. Lattenberg, J. Misurec, "Generalized Design Method for Voltage-Controlled Current-Mode Multifunction Filters," in *Proc. 16th Telecommunications Forum TELFOR 2008*, Belgrade, Serbia, pp. 400–403, 2008.
- [35] D. Biolek, R. Senani, V. Biolkova, Z. Kolka, "Active Elements for Analog Signal Processing: Classification, Review, and New Proposals," *Radioengineering*, vol. 17, no. 4, 2008.
- [36] J. Sirirat, D. Prasertsom, W. Tangsrirat, "High-Output-Impedance Current-Mode Electronically Tunable Universal Filter Using Single CFTA," in *Proc. Int. Symp. Communications and Information Technologies - ISCIT*, Tokyo, Japan, pp. 200–203, 2010.
- [37] N. Herencsar, J. Koton, K. Vrba, "Realization of Current-Mode KHN-Equivalent Biquad Using Current Follower Transconductance Amplifiers (CFTAs)," *IEICE Transactions on Fundamentals of Electronics Communications and Computer Sciences*, vol. E93, pp. 1816–1819, 2010.
- [38] W. Tangsrirat, "Novel current-mode and voltage-mode universal biquad filters using single CFTA," *Indian J. Engineering and Materials Science*, vol. 17, pp. 99–104, 2010.
- [39] J. Sirirat, W. Tangsrirat, W. Surakampon-torn, "Voltage-mode electronically tunable universal filter employing single CFTA," in *Proc. Int. Conf. Electrical Engineering/Electronics Computer Telecommunications and Information Technology - ECTI-CON*, Chaing Mai, pp. 759–763, 2010.
- [40] W. Tangsrirat, "Single-input three-output electronically tunable universal current-mode filter using current follower transconductance amplifiers," *Int. J. Electronics and Communications - AEU*, vol. 65, pp. 783–787, 2011.
- [41] J. Satansup, T. Pukkalanun, W. Tangsrirat, "Current-Mode KHN Biquad Filter Using Modified CFTAs and Grounded Capacitors," in *Proc. Int. MultiConf. of Engineers and Computer Scientists - IMECS*, Hong Kong, vol. II, 2011.
- [42] D. Duangmalai, A. Noppakarn, W. Jaikla, "Electronically Tunable Low-Component-Count Current-Mode Biquadratic Filter Using CFTAs," in *Proc. Int. Conf. Information and Electronics Engineering - IPCSIT*, Singapore, vol. 6, pp. 263–267, 2011.
- [43] J. Satansup, W. Tansrirat, "Realization of current-mode KHN-equivalent biquad filter using ZC-CFTAs and grounded capacitors," *Indian J. Pure and Applied Physics*, vol. 49, pp. 841–846, 2011.
- [44] J. Satansup, W. Tansrirat, "Single-Input Five-Output Electronically Tunable Current-Mode Biquad Consisting of Only ZC-CFTAs and Grounded Capacitors," *Radioengineering*, vol. 20, no. 3, pp. 650–655, 2011.
- [45] W. Jaikla, S. Lawanwisut, M. Sirirprucyanun, P. Prommee, "A Four-Inputs Single-Output Current-Mode Biquad Filter Using a Minimum Number of Active and Passive Components," in *Proc. Int. Conf. Telecommunications and Signal Processing - TSP*, Prague, Czech Republic, pp. 378–381, 2012.
- [46] W. Tangsrirat, "Active-C Realization on nth-order Current-Mode Allpole Lowpass Filters Using CFTAs," in *Proc. Int. MultiConf. of Engineers and Computer Scientists - IMECS*, Hong Kong, vol. II, 2012.
- [47] P. Suwanjan, W. Jaikla, "CFTA Based MISO Current-mode Biquad

- Filter," in *Proc. Int. Conf. Recent Trends in Circuits, Systems, Multimedia and Automatic Control*, pp. 93–97, 2012.
- [48] M. Kumngern, "Electronically tunable current-mode universal bi-quadratic filter using a single CCCFTA," in *Proc. Int. Symp. Circuits and Systems - ISCAS*, Seoul, South Korea, pp. 1175–1178, 2012.
- [49] B. Singh, A.K. Singh, R. Senani, "New Universal Current-mode Biquad Using Only Three ZC-CFTAs," *Radioengineering*, vol. 21, no. 1, pp. 273–280, 2012.
- [50] S. Lawanwisut, M. Siripruchyanun, "A Current-mode Multifunction Biquadratic Filter Using CFTAs," *J. of KMUTNB*, vol. 22, no. 3, pp. 479–485, 2012.
- [51] W. Tangsrirat, P. Mongkolwai, T. Pukkalanun, "Current-mode high-Q bandpass filter and mixed-mode quadrature oscillator using ZC-CFTAs and grounded capacitors," *Indian J Pure and Applied Physics*, vol. 50, pp. 600–607, 2012.
- [52] X. Nie, Z. Pan, "Multiple-input single-output low-input and high-output impedance current-mode biquadratic filter employing five modified CFTAs and only two grounded capacitors," *Microelectronics Journal*, vol. 44, no. 9, pp. 802–806, 2013.
- [53] W. Tangsrirat, "Gm-Realization of Controlled-Gain Current Follower Transconductance Amplifier," *The Scientific World Journal*, vol. 2013, pp. 1–8, doi:10.1155/2013/201565, 2013.
- [54] R.S. Tomar, C. Chauhan, S.V. Singh, D.S. Chauhan, "Current-Mode Active-C Biquad Filter Using Single MO-CCCFTA," in *Proc. Int. Conf. Recent Trends in Computing and Communication Engineering - RTCCE*, pp. 259–262, 2013.
- [55] W. Tangsrirat, S. Unhavanich, "Signal flow graph realization of single-input five-output current-mode universal biquad using current follower transconductance amplifiers," *Rev. Roum. Sci. Techn. - Electrotechn. et Energ.*, vol. 59, no. 2, pp. 183–191, 2014.
- [56] N. Herencsar, J. Koton, K. Vrba, "Electronically Tunable Phase Shifter Employing Current-Controlled Current Follower Transconductance Amplifiers (CCCFTAs)," in *Proc. 32nd Int. Conf. Telecommunications and Signal Processing - TSP*, Budapest, Hungary, pp. 54–57, 2009.
- [57] P. Mongkolwai, T. Dumawipata, W. Tangsrirat, "Current-Mode Quadrature Oscillator Employing ZC-CFTA Based First-Order Allpass Sections," in *Int. Conf. Modeling and Simulation Technology*, Tokyo, Japan, pp. 472–475, 2011.
- [58] T. Nakyoy, W. Jaikla, "Resistorless First-Order Current-Mode Allpass Filter Using Only Single CFTA and Its Application," in *Proc. IEEE Int. Symp. Electronic Design, Test and Application - DELTA*, Queenstown, doi: 10.1109/DELTA.2011.28, pp. 105–109, 2011.
- [59] K. Intawichai, W. Tangsrirat, "Signal flow graph realization of nth-order current-mode allpass filters using CFTAs," in *Proc. Int. Conf. Electrical Engineering/Electronics Computer Telecommunications and Information Technology - ECTI-CON*, Krabi, doi:10.1109/ECTICon.2013.6559519 pp. 1–6, 2013.
- [60] A. Iamarejin, S. Maneewan, P. Suwanjan, W. Jaikla, "Current-mode variable current gain first-order allpass filter employing CFTAs," *Przegląd Elektrotechniczny*, vol. 89, no. 2a, pp. 238–241, 2013.
- [61] A. Lahiri, "Resistor-less mixed-mode quadrature sinusoidal oscillator," *Int. J. Computer and Electrical Engineering*, vol. 2, no. 1, pp. 63–66, 2010.
- [62] N. Herencsar, K. Vrba, J. Koton, A. Lahiri, "Realizations of single-resistance-controlled quadrature oscillators using a generalized current follower transconductance amplifier and a unity-gain voltage-follower," *Int. J. Electronics*, vol. 97, no. 8, pp. 897–906, 2010.
- [63] S. Maneewan, B. Sreewirote, W. Jaikla, "A Current-mode Quadrature Oscillator Using a Minimum Number of Active and Passive Components," in *Proc. IEEE Int. Conf. Vehicular Electronics and Safety - ICVES*, Beijing, doi:10.1109/ICVES.2011.5983835, pp. 312–315, 2011.
- [64] M. Kumngern, U. Torteanchai, "A Current-Mode Four-Phase Third-Order Quadrature Oscillator Using a MCCCFTA," in *Proc. IEEE Int. Conf. Cyber Technology in Automation, Control and Intelligent Systems*, Bangkok, Thailand, pp. 156–159, 2012.
- [65] D. Prasertsom, W. Tangsrirat, "Current Gain Controlled CFTA and Its Application to Resistorless Quadrature Oscillator," in *Proc. Int. Conf. Electrical Engineering/Electronics Computer Telecommunications and Information Technology - ECTI-CON*, Phetchaburi, doi: 10.1109/ECTI-Con.2012.6254271, pp. 1–4, 2012.
- [66] P. Uttaphut, "Realization of Electronically Tunable Current-Mode Multiphase Sinusoidal Oscillators using CFTAs," *World Academy of Science, Engineering and Technology*, vol. 69, pp. 719–722, 2012.
- [67] Y.A. Li, "Electronically tunable current-mode biquadratic filter and four-phase quadrature oscillator," *Microelectronics Journal*, vol. 45, no. 3, pp. 330–335, 2014.
- [68] P. Mongkolwai, W. Tangsrirat, "CFTA-based current multiplier/divider circuit," in *Proc. IEEE Int. Symp. Intelligent Signal Processing and Communications Systems - ISPACS*, Chiang Mai, doi: 10.1109/ISPACS.2011.6146074, pp. 1–4, 2011.
- [69] P. Silapan, C. Chanapromma, "Multiple Output CFTAs (MO-CFTAs)-based Wide-range Linearly/Electronically Controllable Current-mode Square-rooting Circuit," in *Proc. IEEE Int. Symp. Intelligent Signal Processing and Communications Systems - ISPACS*, Chiang Mai, doi: 10.1109/ISPACS.2011.6146152, pp. 1–4, 2011.
- [70] P. Silapan, C. Chanapromma, T. Worachak, "Realization of Electronically Controllable Current-mode Square-rooting Circuit Based on MO-CFTA," *World Academy of Science, Engineering and Technology*, vol. 58, pp. 493–496, 2011.
- [71] W. Kongnun, A. Aurasopon, "A Novel Electronically Controllable of Current-Mode Level Shifted Multicarrier PWM Based on MO-CFTA," *Radioengineering*, vol. 22, no. 3, pp. 907–915, 2013.
- [72] W. Kongnun, P. Silapan, "A Single MO-CFTA Based Electronically/Temperature Insensitive Current-mode Half-wave and Full-wave Rectifiers," *Advances in Electrical and Electronic Engineering*, vol. 11, no. 4, pp. 275–283, 2013.
- [73] N. Herencsar, J. Koton, K. Vrba, A. Lahiri, "Floating Simulators Based on Current Follower Transconductance Amplifiers (CFTAs)," *Advances in Communications, Computers, Systems, Circuits and Devices*, pp. 23–26, 2010.
- [74] N. Herencsar, J. Koton, K. Vrba, O. Cicekoglul, "New Active-C Grounded Positive Inductance Simulator Based on CFTAs," in *Proc. 33th Int. Conf. Telecommunications and Signal Processing - TSP*, Baden bei Wien, Austria, pp. 35–37, 2010.
- [75] M. Fakhfakh, M. Pierzchala, B. Rodanski, "An Improved Design of VCCS-Based Active Inductors," in *Proc. Int. Conf. on Synthesis, Modeling, Analysis and Simulation Methods and Applications to Circuit Design - SMACD*, Seville, pp. 101–104, doi: 10.1109/SMACD.2012.6339427, 2012.
- [76] N. Herencsar, A. Lahiri, J. Koton, K. Vrba, R. Sotner, "New Floating Lossless Inductance Simulator Using Z-copy Current Follower Transconductance Amplifier," in *Proc. 22nd Int. Conf. Radioelektronika*, Brno, Czech Republic, pp. 93–96, 2012.
- [77] D. Siriphot, S. Maneewan, W. Jaikla, "Single Active Element Based Electronically Controllable Grounded Inductance Simulator," in *Proc. IEEE Int. Conf. Biomedical Engineering - BMEiCON*, Amphur Muang, pp. 1–4, doi: 10.1109/BMEiCon.2013.6687724, 2013.
- [78] Y.-A. Li, "A series of new circuits based on CFTAs," *Int. J. Electronics and Communications - AEU*, vol. 66, pp. 587–592, 2012.
- [79] M. Venclovsky, *Transform-based filter design technique based on passive structures*, Master's thesis, Brno University of Technology, 2009.
- [80] W.-K. Chen, *The Circuits and Filters Handbook*, New York, CRC Press, 2003, 2nd edition, ISBN 0-8493-0912-3.
- [81] T. Deliyannis, Y. Sun, J.K. Fidler, *Continuous-Time Active Filter Design*, New York, CRC Press, 1999, ISBN 0-8493-2573-0.